

Dependence of electronic polarization on octahedral rotations in TbMnO_3 from first principles

Andrei Malashevich* and David Vanderbilt

Department of Physics & Astronomy, Rutgers University, Piscataway, NJ 08854-8019, USA

(Dated: November 4, 2018)

The electronic contribution to the magnetically induced polarization in orthorhombic TbMnO_3 is studied from first principles. We compare the cases in which the spin cycloid, which induces the electric polarization via the spin-orbit interaction, is in either the b - c or a - b plane. We find that the electronic contribution is negligible in the first case, but much larger, and comparable to the lattice-mediated contribution, in the second case. However, we show that this behavior is an artifact of the particular pattern of octahedral rotations characterizing the structurally relaxed $Pbnm$ crystal structure. To do so, we explore how the electronic contribution varies for a structural model of rigidly rotated MnO_6 octahedra, and demonstrate that it can vary over a wide range, comparable with the lattice-mediated contribution, for both b - c and a - b spirals. We introduce a phenomenological model that is capable of describing this behavior in terms of sums of symmetry-constrained contributions arising from the displacements of oxygen atoms from the centers of the Mn-Mn bonds.

PACS numbers: 75.80.+q, 77.80.-e

I. INTRODUCTION

Multiferroic materials have been the subject of much excitement because they exhibit many interesting properties and phenomena.^{1,2,3,4,5,6} There are two basic scenarios for the coexistence of two order parameters in a single phase. Either the two instabilities can both be present independently, or one can induce the other via some coupling mechanism. We are concerned here with magnetoelectric (ME) materials of the latter type, in which the primary instability is magnetic, and the resulting magnetic order induces an electric polarization. Such magnetically-induced (improper) ferroelectrics can be expected to display strong ME couplings, e.g., a strong dependence of the electric polarization on applied magnetic field, or of the magnetization on the applied electric field.⁶ They could be extremely useful in many technological applications, but most of the materials discovered to date either have too small of a ME coupling, or only operate at impractically low temperatures. Thus, it is essential to understand their coupling mechanisms more fully in order to design new materials with enhanced ME effects that can operate at higher temperatures.

Among the best studied of the magnetically induced ferroelectrics are orthorhombic rare-earth manganites, o - RMnO_3 .^{5,7,8,9,10,11,12,13,14} Intensive experimental and theoretical studies have clarified many questions regarding the origin of ferroelectricity in these compounds. In HoMnO_3 and YMnO_3 , the collinear E -type antiferromagnetic (AFM) spin order induces a polarization through the exchange striction mechanism.^{7,8,9} In TbMnO_3 and DyMnO_3 , in contrast, the polarization appears with the onset of spiral magnetic order^{10,11} as a consequence of the spin-orbit interaction.⁵

On a microscopic level, the appearance of the polarization can result either from a change in electron charge density that would occur even with ionic coordi-

ates clamped (the purely electronic contribution), or from displacements of the ions away from their centrosymmetric positions as a result of magnetically induced forces (lattice contributions). In any theoretical analysis of such materials, it is important to distinguish between these two contributions and to calculate them separately in order to understand which microscopic mechanisms are responsible for the appearance of the polarization.^{8,9,12,13,14} Regarding the o - RMnO_3 materials having the cycloidal spin structure, Xiang *et al.*¹² and we^{12,13} have demonstrated that in TbMnO_3 the electronic contribution to the polarization is much smaller than the lattice contribution when the spin spiral is lying in the b - c plane. For this reason, our previous work^{13,14} focused on a detailed analysis of the lattice contribution, while the electronic contribution was not studied carefully. The mode decomposition of the lattice contribution¹³ and its dependence on the spin spiral wave vector¹⁴ revealed that the next-nearest-neighbor spin interactions are important not only for the formation of the spin spiral itself, but also for the induced polarization.

Although in this particular case the lattice contribution is dominant, it is not clear how general this result is. Picozzi *et al.*⁸ showed that for orthorhombic HoMnO_3 , in which the polarization is induced by collinear E -type AFM order, the electronic contribution to the polarization is of the same order as the lattice contribution. Although the mechanism of polarization induction in HoMnO_3 is different from that in TbMnO_3 , there is no *a priori* reason why the electronic contribution should be negligible in TbMnO_3 . In fact, the first-principles study by Xiang *et al.*¹² found that if the spin spiral lies in the a - b plane, the electronic contribution to the polarization is of the same order of magnitude as the lattice contribution.

In this work, we study the polarization induced by the a - b -plane spin spiral and show that this case differs sig-

nificantly from the case of the b - c -plane spiral. We focus mainly on the electronic contribution, analyzing it carefully for both cases by considering how it varies for a structural model of rigidly rotated MnO_6 octahedra. We confirm the finding of Xiang *et al.*¹² that the purely electronic contribution to the polarization is not negligible for the case of the a - b spiral. Indeed, we find it to be quite sensitive to the choice of the calculation parameters, as well as on the octahedral rotation angles. Even for the case of the b - c spiral, we find that the electronic contribution can be quite significant if the octahedral rotation angles are varied away from the equilibrium values.

We also construct a phenomenological model based on a symmetry analysis of the spin-orbit induced electronic dipoles associated with centrosymmetry-compatible oxygen displacements relative to the centers of the Mn-Mn bonds, finding that it is essential to take the Jahn-Teller orbital ordering into account from the outset. This model shows that b - c and a - b spin spirals need not be similar in terms of how the polarization is induced. Our work implies that the electronic contribution to the polarization is generically expected to be much larger than was found for the specific case of the relaxed b - c spiral state in TbMnO_3 , emphasizing the importance of considering both electronic and lattice mechanisms in any future theoretical studies of this class of materials.

The rest of the paper is organized as follows. In Sec. II we compare the electric polarization computed for fully relaxed TbMnO_3 with the spin spiral lying in the b - c and a - b planes for several values of the on-site Coulomb energy U in the LDA+ U framework. In Sec. III we focus on the study of the purely electronic contribution to the polarization in the context of a structural model of TbMnO_3 in which the Mn and O ions form rigid octahedra. The dependence of the Berry-phase polarization on octahedral rotations is studied in Sec. III A, while in Sec. III B we develop a symmetry-based phenomenological model in an attempt to explain the observed results. We discuss our findings in Sec. IV, and give a brief summary in Sec. V.

II. SPIN SPIRALS IN THE b - c AND a - b PLANES

A spiral (or, more precisely, “cycloidal”¹⁵) spin structure forms in TbMnO_3 in the b - c -plane below ~ 27 K with the polarization lying along the \hat{c} axis.¹⁰ However, a sufficiently strong magnetic field applied along the \hat{b} direction causes the polarization to change its direction from \hat{c} to \hat{a} (“electric polarization flop”). It was suggested, and recently confirmed,¹⁶ that this polarization flop results from the change of the spin spiral from the b - c to the a - b plane (“spin flop”); the polarization simply follows the spin spiral. We shall refer to these two magnetic states as the ‘ b - c spiral’ and ‘ a - b spiral’. The former is incommensurate with a wavevector $k_s \simeq 0.28$, while the latter is commensurate with $k_s = 1/4$.

In this section we first review the main results of our

previous calculations^{13,14} of the polarization induced by the b - c spiral. We then present our new calculations for the case of the a - b spiral, and compare these two cases.

We use a 60-atom supercell consisting of three $Pbnm$ unit cells, corresponding to a spin-spiral wave vector of $k_s = 1/3$, for both the a - b and b - c spirals. Although $k_s = 1/4$ experimentally for the a - b spiral, the use of four unit cells would be more computationally demanding, and the consistent use of $k_s = 1/3$ facilitates comparisons between the two cases. (An additional reason why $k_s = 1/3$ is more convenient will be mentioned at the end of Sec. III B.)

Our electronic-structure calculations are carried out using a projector augmented-wave^{17,18} method implemented in the VASP code package.¹⁹ Since the local-density approximation (LDA) gives a metallic state for TbMnO_3 , we use on-site Coulomb corrections (LDA+ U) in a rotationally invariant formulation.²⁰ The electric polarization is computed using the Berry-phase method.²¹

In our previous work on the b - c spiral,^{13,14} the structural relaxation was performed in the absence of spin-orbit interaction (SOI), and we confirmed that no polarization is induced by the magnetic order in this case. In the presence of SOI, an electric polarization was found to appear. We decomposed it into electronic and lattice contributions by first keeping the ionic positions frozen at their centrosymmetric values while computing P , and then by repeating the calculation after allowing ions to relax. We found the electronic and lattice contributions to be $P_{\text{elec}} = 32 \mu\text{C}/\text{m}^2$ and $P_{\text{latt}} = -499 \mu\text{C}/\text{m}^2$ respectively. This result demonstrated that the lattice mechanism dominates over the purely electronic one for the b - c spiral in TbMnO_3 .

The polarization values quoted above were calculated using $U = 1$ eV to match the experimental band gap.¹³ We also studied the effect of the choice of U parameter (in a reasonable range of values from 1 eV to 4 eV) on the induced polarization and coupling mechanism.¹⁴ We found that while the absolute value of P becomes somewhat smaller with larger U , the qualitative mechanism of polarization induction remains the same.

In the case of the a - b spiral, we have now performed similar calculations of the polarization for the same set of U values from 1 eV to 4 eV. Table I shows the results for $U = 1$ eV and $U = 4$ eV. For these values we proceeded as in our previous work, taking a reference crystal structure that was fully relaxed in the absence of SOI, computing the SOI-induced electric polarization P^{elec} and ionic forces, and then using the latter, together with the computed Born charges and force-constant matrix elements, to predict P^{latt} . (For intermediate U we only computed P^{elec} , and did so in a simplified manner by using the reference crystal structure that was relaxed at $U = 1$ eV, finding $P^{\text{elec}} = 691$ and $397 \mu\text{C}/\text{m}^2$ for $U = 2$ and 3 eV, respectively. These values are intermediate between the values for $U = 1$ and $U = 4$ eV as expected.)

For comparison, we also show in Table I the results of similar calculations by Xiang *et al.*,¹² who used $U = 2$ eV

TABLE I: Purely electronic, lattice, and total polarizations along the \hat{c} and \hat{a} axes for the b - c and a - b spirals respectively. Results at $U_{\text{Mn}} = 2\text{eV}$ (and also using $U_{\text{Tb}} = 6\text{eV}$) from Ref. 12 are shown for comparison.

spiral	U_{Mn} (eV)	P^{elec} ($\mu\text{C}/\text{m}^2$)	P^{latt} ($\mu\text{C}/\text{m}^2$)	P^{tot} ($\mu\text{C}/\text{m}^2$)
b - c	1	32	-499	-467
	4	-14	-204	-218
	2^a	1^a	-425^a	-424^a
a - b	1	1530	-790	740
	4	174	-197	-23
	2^a	331^a	-462^a	-131^a

^aFrom Ref. 12.

on the Mn sites. However, their results are not directly comparable with ours, as they also included Tb f electrons, with $U_{\text{Tb}} = 6\text{eV}$ on the Tb sites. In the b - c spiral case, as we mentioned before, the results do not depend strongly on the choice of U . Comparing in this case the results of Xiang *et al.* with our results for $U = 1\text{eV}$, we find an agreement in that the purely electronic contribution is negligible, and the total polarization values agree with each other within 10%. However, in the a - b spiral case there is no such agreement, which is perhaps not surprising in view of the very strong sensitivity of the polarization to the value of U , as can be seen clearly in the table. It may also result in part from other factors, such as the different treatment of f electrons in the two calculations, or the fact that they used a generalized-gradient (GGA) exchange-correlation while we used LDA. Nevertheless, a point in common is that both calculations predict that the electronic contribution is comparable or even larger than the lattice one for the a - b spiral. This leads us to conclude that the dominance of the lattice contribution that was found earlier for the case of b - c spiral is not a general phenomenon, but was special to that case.

For the b - c spiral, the theoretical values in Table I are in satisfactory agreement with the value of $\sim -600\mu\text{C}/\text{m}^2$ found experimentally.¹⁰ However, for the case of the a - b spiral, the comparison is more problematic. Our computed polarization of $740\mu\text{C}/\text{m}^2$ compares very poorly with the experimental value of $\sim -300\mu\text{C}/\text{m}^2$ obtained by Yamasaki *et al.* for the related $\text{Gd}_{0.7}\text{Tb}_{0.3}\text{MnO}_3$ system.²² However, as we shall discuss in Sec. IV, the polarization depends sensitively on the octahedral tilting angles, which may differ significantly for $\text{Gd}_{0.7}\text{Tb}_{0.3}\text{MnO}_3$. Experiments on the a - b spiral in the TbMnO_3 system itself are somewhat ambiguous regarding both the sign and the magnitude of the polarization.¹⁰

Note that the magnitude of the electronic contribution in the case of the a - b spiral falls rapidly with increasing U . Our calculations show that the band gap increases almost linearly with U . Fig. 1 shows the electronic contribution to the polarization for both a - b and b - c spi-

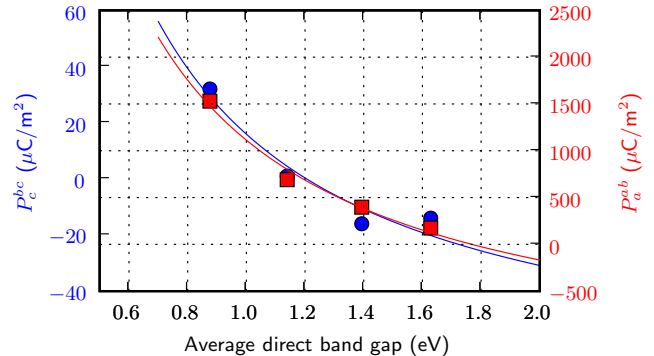


FIG. 1: (Color online.) Dependence of electronic contribution to the polarization on the average direct band gap for the b - c spiral (circles, scale at left) and a - b spiral (squares, scale at right) when varying U .

als plotted versus the average direct band gap. One can see from the plot that the polarization is roughly inversely proportional to the gap, up to a constant shift. A heuristic rationalization of this behavior can be given as follows. If we consider the *derivative* of the polarization with respect to ionic displacements, which is the Born effective charge, we know that this quantity can be expressed within density-functional perturbation theory in a Kubo-Greenwood form involving a sum over terms that are inversely proportional to the differences of the eigenenergies of the unoccupied and occupied states.²³ The largest contributions are expected to come from the smallest energy denominators associated with states near the valence and conduction edges, so the overall sum should roughly scale inversely with the direct band gap. The same applies to other derivatives of the polarization, such as the dielectric susceptibility. If the derivatives of P have this behavior, it is not very surprising to find that the polarization itself has a similar behavior.

In view of the results discussed above, the central question arises: Why are the cases of the a - b and b - c spiral so different? In the remainder of this paper, we attempt to shed some light on this question. For this purpose, we limit ourselves to a discussion of the purely electronic contribution to the polarization. We shall discuss at some length the dependence of the electronic polarization on atomic displacements, but only for displacement patterns that preserve inversion symmetry, such as those resulting from octahedral tilting in the $Pbnm$ crystal structure.

III. MODELING OF P_{elec}

A. Structural model with rigid MnO_6 octahedral rotations

To obtain a better understanding of the mechanism of the electronic contribution to the polarization, we con-

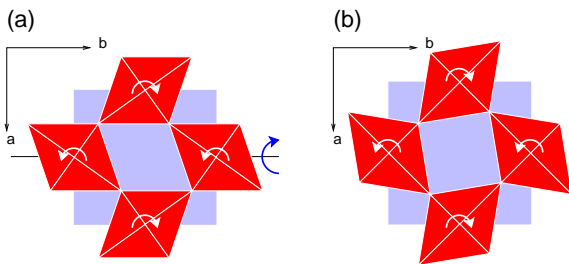


FIG. 2: (Color online.) Two initial configurations considered in the model of rigid MnO_6 octahedra. Rotations about \hat{c} and \hat{b} axes are indicated by white and dark blue curved arrows respectively. (a) Structure 1, which matches the physical $Pbnm$ structure fairly closely. (b) Structure 2, with a fictitious pattern of octahedral rotations around the \hat{c} axis only.

consider a simplified structural model in which the crystal structure is composed of rigid corner-linked MnO_6 octahedra, with the Tb ions remaining at their high-symmetry $(0,0,1/4)$ Wyckoff coordinates. We then rotate the MnO_6 octahedra and study how the polarization depends on the rotation angles. All calculations within this model are done with $U = 1$ eV. While the values of the polarization computed with this U may not be realistic for the case of the a - b spiral, as discussed above, at this point we are interested in understanding the origins and behavior of the polarization, rather than making direct comparisons to experiment. Also, we want to compare the results with previous calculations,^{13,14} most of which were done at $U = 1$ eV.

Actually, before we even apply the rotations, we must first apply a Jahn-Teller (JT) distortion. Mn^{3+} has a d^4 configuration in which the three majority-spin t_{2g} states are filled and the majority-spin e_g levels are half-filled. The system is thus metallic in the absence of the JT distortion; introducing it splits the e_g levels and opens a gap, driving the system insulating. In our model, we take the JT distortion into account by pre-deforming the MnO_6 octahedra such that the ratio of longest to intermediate (along c) to shortest bonds lengths is 1.124:1.004:1, where these ratios have been extracted from our earlier first-principles calculations carried out with $U = 1$ eV.¹³

We then apply rotations to the octahedra. In $Pbnm$ symmetry the rotations can be described as $(a^- a^- b^+)$ in the Glazer notation,²⁴ meaning that out-of-phase and in-phase alternating rotations occur around $[110]$ and $[001]$ axes respectively in the original cubic-perovskite Cartesian frame. In the conventional frame¹⁰ used here, these correspond to the \hat{b} and \hat{c} axes respectively, and the spin-spiral wave vector propagates along \hat{b} .

In general, a different order of application of rotations leads to different final configurations, because rotations do not commute. Therefore, when describing the TbMnO_3 system in terms of MnO_6 octahedral rotations, one should carefully specify the meaning of the rotations

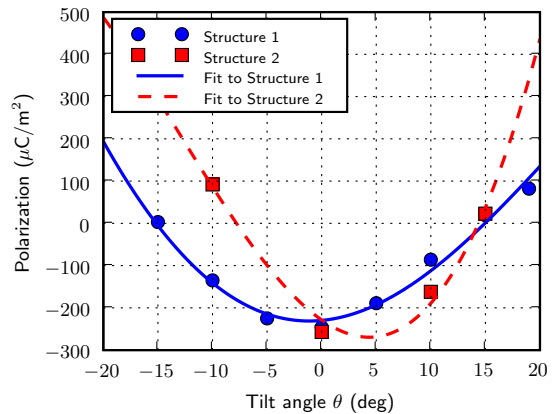


FIG. 3: (Color online) For b - c spiral, the dependence of the electronic contribution to the polarization on θ , the angle of rotation of the MnO_6 octahedra about the \hat{b} or \hat{c} axis for Structure 1 or 2 respectively. (For the former, the rotation angle around \hat{c} is $\theta/1.64$; see text for details.) Symbols: first-principles calculations. Curves: result of the fit to the phenomenological model of Sec. III B.

and their order. For example, if we start with the ideal perovskite configuration and induce the Jahn-Teller distortion, we can arrive at several possible initial configurations as shown in Fig. 2. If we apply $(a^- a^- b^+)$ rotations to the configuration shown in Fig. 2(b), regardless of the order of rotations, the final structure will not have $Pbnm$ symmetry. However, applying a rotation around \hat{b} followed by a rotation around \hat{c} to the configuration shown in Fig. 2(a), we will preserve the $Pbnm$ symmetry.

Fitting the angles of rotation to the relaxed structure, we find the rotation angles around \hat{b} and \hat{c} to be approximately 19.0° and 11.6° respectively. We thus constrain the ratio between these two angles to be 1.64, and treat the angle θ around the \hat{b} axis as the independent variable. We calculate the polarization for both the a - b and b - c spirals for a range of rotation angles $-15^\circ < \theta < 20^\circ$. We also made several calculations for the initial configuration shown in Fig. 2(b), where the octahedra were rotated only around \hat{c} . To distinguish between the two sets of calculations, we will refer to them as ‘Structure 1’ and ‘Structure 2’ respectively.

The results of the calculations are presented in Figs. 3 and 4. Recall that all structures considered here have inversion symmetry, so that the Berry-phase calculations give us the purely electronic contribution to the polarization induced by the SOI. These calculations reveal that even in the case of the b - c spiral, the electronic contribution to the polarization spans a wide range of values ($\sim 300 \mu\text{C}/\text{m}^2$), depending on the octahedral rotations. This is yet another indication that this contribution is negligible in the relaxed b - c spiral structure only by coincidence.

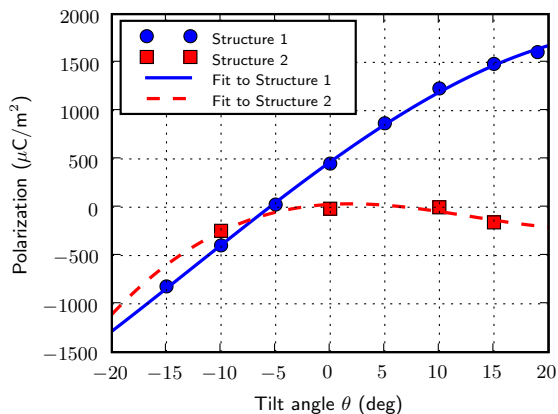


FIG. 4: (Color online) For a - b spiral, the dependence of the electronic contribution to the polarization on θ , the angle of rotation of the MnO_6 octahedra about the $\hat{\mathbf{b}}$ or $\hat{\mathbf{c}}$ axis for Structure 1 or 2 respectively. (For the former, the rotation angle around $\hat{\mathbf{c}}$ is $\theta/1.64$; see text for details.) Symbols: first-principles calculations. Curves: result of the fit to the phenomenological model of Sec. III B.

B. Phenomenological model

To find out whether the observed dependence of the polarization on octahedral rotations can be explained within some relatively simple model, we decided to analyze the possible contributions coming from each nearest-neighbor Mn–O–Mn triplet. Our notation is as follows. We use $\hat{\mathbf{a}}$, $\hat{\mathbf{b}}$, and $\hat{\mathbf{c}}$ for the unit vectors in the global Cartesian frame of Fig. 2. We also attach a local Cartesian frame to each Mn–O–Mn triplet as illustrated in Fig. 5(a), reserving $\hat{\mathbf{z}} = \hat{\mathbf{e}}_{12}$ (the unit vector pointing from Mn1 to Mn2), while $\hat{\mathbf{x}}$ and $\hat{\mathbf{y}}$ are chosen to form a right-handed triad with $\hat{\mathbf{z}}$ such that $\hat{\mathbf{x}}$ lies in the a - b plane. The origin of this frame is located in the middle of the Mn–Mn bond. The angle between $\hat{\mathbf{e}}_{12}$ and the spin-spiral wavevector direction $\hat{\mathbf{b}}$ is denoted by α , so that $\cos \alpha = \hat{\mathbf{z}} \cdot \hat{\mathbf{b}}$. For the vertical bonds parallel to $\hat{\mathbf{c}}$, the local and global Cartesian frames coincide and $\alpha = \pi/2$.

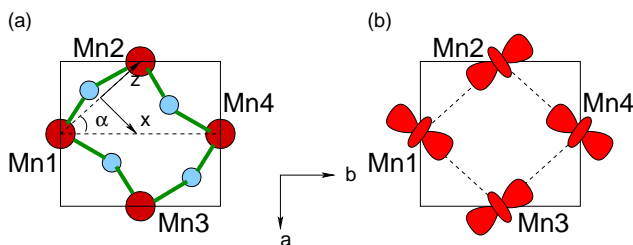


FIG. 5: (a) Local (x, y, z) and global (a, b, c) coordinate frames. (b) Orbital ordering in TbMnO_3 . The $d_{3x^2-r^2}/d_{3y^2-r^2}$ orbitals are aligned along the longest Mn–O bonds. Orbital order is uniform along the $\hat{\mathbf{c}}$ axis.

TABLE II: Classification of several quantities by their behavior under the mirror symmetries M_x and M_y : products of the spin components of two neighboring spins \mathbf{S}_1 and \mathbf{S}_2 , components of oxygen displacement vectors \mathbf{u} , and components of the polarization vector \mathbf{P} .

M_x	M_y				
+1	+1	$S_{1x}S_{2x}, S_{1y}S_{2y}, S_{1z}S_{2z}$	u_z	u_x^2, u_y^2, u_z^2	P_z
+1	-1	$S_{1y}S_{2z}, S_{1z}S_{2y}$	u_y	$u_y u_z$	P_y
-1	+1	$S_{1x}S_{2z}, S_{1z}S_{2x}$	u_x	$u_x u_z$	P_x
-1	-1	$S_{1x}S_{2y}, S_{1y}S_{2x}$		$u_x u_y$	

Our goal is to find dipole moments allowed by symmetry for each Mn–O–Mn bond, viewed in isolation. To find the total polarization, we need to transform these dipole moments back into the global Cartesian frame, average them over the spin-spiral period, and sum the contributions from all Mn–O–Mn bonds in the 20-atom unit cell. One can show that there is no contribution to the polarization coming from the vertical bonds by using the fact that the magnetic moments on the Mn sites are collinear for these bonds. Therefore, we focus henceforth only on the bonds lying in the a - b plane.

We expand the dipole moment of each Mn–O–Mn triplet in (i) bilinear products of spin components on the two Mn sites, and (ii) powers of oxygen displacements related to the MnO_6 octahedral rotations. We invoke symmetry to determine the appropriate terms in this expansion, as follows. Consider the configuration shown in Fig. 2(b). The Mn–O–Mn bonds have two mirror symmetries, M_x and M_y . Note that the bond does not have inversion symmetry because the JT distortion leads to an orbital ordering pattern, shown schematically in Fig. 5(b), which breaks M_z . We emphasize that it is essential to take this JT distortion, and the associated orbital order, into account. If instead one attempts to use a JT-free perovskite structure as the reference for such an expansion, one finds the reference system to be metallic, so that the electric polarization cannot even be defined. Therefore, it is first necessary to establish an orbitally-ordered insulating state, and only then expand the electronic dipoles in lattice displacements away from that state. Indeed, we initially attempted to derive a model built on the erroneous assumption of inversion symmetry for Mn–O–Mn bonds in a reference structure without JT distortions, but we could not arrive at a satisfactory low-order expansion that could simultaneously fit the data for both a - b and b - c spirals.

We classify the products of spin components by their behavior under the two mirror symmetries, as tabulated in Table II. We can then systematically expand the po-

larization in powers of displacements (u_x, u_y, u_z) as

$$\begin{aligned}
P_x = & A_{xz}^{(0)} S_{1x} S_{2z} + A_{zx}^{(0)} S_{1z} S_{2x} \\
& + [A_{xx}^{(1)} S_{1x} S_{2x} + A_{yy}^{(1)} S_{1y} S_{2y} + A_{zz}^{(1)} S_{1z} S_{2z}] u_x \\
& + [A_{xy}^{(1)} S_{1x} S_{2y} + A_{yx}^{(1)} S_{1y} S_{2x}] u_y \\
& + [A_{xz}^{(1)} S_{1x} S_{2z} + A_{zx}^{(1)} S_{1z} S_{2x}] u_z + \dots \quad (1)
\end{aligned}$$

Here we show only the terms that appear at zero and first order in u because the expression rapidly becomes tedious at higher order, but our analysis also includes all second-order terms. Similar expressions can be written for P_y and P_z . Projecting these contributions on the $\hat{\mathbf{a}}$, $\hat{\mathbf{b}}$, and $\hat{\mathbf{c}}$ axes and averaging over the spin-spiral period and all Mn-Mn bonds in the unit cell, we arrive at

$$\begin{aligned}
P_c^{(b-c)} = \sin \phi \{ & C_0 + C_x u_x + C_z u_z + C_{xx} u_x^2 + C_{yy} u_y^2 \\
& + C_{zz} u_z^2 + C_{xz} u_x u_z \} \quad (2)
\end{aligned}$$

for the polarization in the case of the b - c spiral, and

$$\begin{aligned}
P_a^{(a-b)} = \sin \phi \{ & A_0 + A_x u_x + A_z u_z + A_{xx} u_x^2 + A_{yy} u_y^2 \\
& + A_{zz} u_z^2 + A_{xz} u_x u_z \} \quad (3)
\end{aligned}$$

in the case of a - b spiral. The coefficients in Eqs. (2-3) are just certain linear combinations of those appearing in Eq. (1) and the corresponding equations for P_y and P_z .

The resulting expressions in Eqs. (2-3) for the polarization may be viewed as simple Taylor expansions in the oxygen displacements from the centers of the Mn-O-Mn bonds. However, some terms are missing because they are forbidden by symmetry. For example, terms linear in u_y vanish after averaging along $\hat{\mathbf{c}}$ because the contribution from any bond in Fig. 5(a) is canceled by the one from the bond above or below. The symmetry also implies that $P_a^{(b-c)} = P_b^{(b-c)} = P_b^{(a-b)} = P_c^{(a-b)} = 0$ after averaging over the spin-spiral period. The factor of $\sin \phi$ comes from averaging the products of spin components over the spin-spiral period. In this model we did not consider next-nearest-neighbor spin interactions, which were shown to play an important role in the dependence of P_c on the magnitude of the wave vector in the b - c spiral case.^{13,14} However, we argue that the contributions to the polarization coming from these interactions will have essentially the same form as Eqs. (2-3), but with $\sin \phi$ replaced by $\sin(2\phi)$. In our particular case $\phi = \pi/3$, so that $\sin \phi = \sin(2\phi)$ and the inclusion of the next-nearest-neighbor interactions will only lead to a renormalization of the coefficients in the expansions.

Eqs. (2-3) have no coefficients in common, showing that within this model there is no connection between the polarization in the b - c and a - b spirals. The results for each spiral case can be fitted independently with seven parameters, whose fitted values are given in Table III. In each of Figs. 3 and 4, the resulting fits are shown as the solid and dashed curves that refer, respectively, to Structures 1 and 2 of Fig. 2(a) and Fig. 2(b). Eqs. (2-3)

TABLE III: Fitted parameters C_i and A_i for the model of Eqs. (2-3) for b - c and a - b spirals respectively. Units are $\mu\text{C}/\text{m}^2$, $\mu\text{C}/\text{m}^2\text{\AA}$, and $\mu\text{C}/\text{m}^2\text{\AA}^2$ for terms of overall order 0, 1, and 2, respectively. Column labels are subscripts i .

	0	x	z	xx	yy	zz	xz
C_i	-285	-3466	211	1297	1143	3263	-30576
A_i	92	-8245	529	555	-1403	361	-33707

clearly provide enough freedom to allow a very good simultaneous fit to the results computed directly from first principles for both structures. If we go back and take the relaxed structures that were obtained directly from the first-principles calculations (for $U=1$ eV and no SOI) and use the present model to evaluate the electronic contribution to the polarization, we obtain $P_c = 1600 \mu\text{C}/\text{m}^2$ and $P_a = 31 \mu\text{C}/\text{m}^2$ for the b - c and a - b spirals, to be compared with values of 1530 and $32 \mu\text{C}/\text{m}^2$ computed directly from first principles, respectively.

IV. DISCUSSION

Our Berry-phase calculations of the electronic contribution to the polarization for various model TbMnO_3 structures, in which rigid MnO_6 octahedra were rotated, show that the polarization in the a - b -spiral case behaves quite differently than for the b - c -spiral case. Not only is the range of values different, but the qualitative dependence of P_{elec} on rotation angles is dissimilar. For the b - c spiral, the polarization shows a parabolic dependence on the rotation angles, while for the a - b case the dependence is almost linear over a wide range of rotation angles. The phenomenological model considered above suggests that, at least from the point of view of symmetry, there is no relation between the b - c spiral and a - b spirals, so that the observed differences should not be very surprising.

Considering that the octahedral rotation angles and oxygen displacements become quite large, we obtain quite good fits of the dependence of the polarization on rotation angles from our expansion of the dipoles on oxygen displacements away from the Mn-Mn bond centers. The observed behavior results from the fact that the coefficients in front of u_x and u_z are much larger in the a - b spiral, while the quadratic coefficients in front of u_{xx} and u_{zz} are much larger in the b - c spiral (see Table III). It still remains to understand how the most important coefficients in the expansion get their values based on some microscopic model of bond hybridization.

If we compare our computed polarization for the relaxed TbMnO_3 structure in the a - b spiral case ($740 \mu\text{C}/\text{m}^2$, see Table I) to the experimental value for $\text{Gd}_{0.7}\text{Tb}_{0.3}\text{MnO}_3$ in Ref. 22 ($\sim -300 \mu\text{C}/\text{m}^2$), we find very poor agreement. However, since Gd has a larger radius than Tb, the MnO_6 octahedra will be less tilted, reducing the electronic contribution to the polarization (see Structure 1 in Fig. 4). This effect may help explain

the observed difference. However, it should also be kept in mind that the strong sensitivity of the polarization to the choice of U in the case of the a - b spiral means that any prediction of the polarization made within the LDA+U framework will have a much larger uncertainty than for the b - c spiral case. The use of linear-response techniques to compute the effective parameters for the LDA+U method²⁵ could thus be appropriate here. However, the very use of the LDA+U method itself may be questionable, and it may be worth exploring the suitability of other methods, such as GW quasiparticle²⁶ or dynamical mean-field theory²⁷ approaches, for computing the polarization in this case.

We have seen that the octahedral rotations can significantly change the polarization. Although we have focused here only on the electronic contribution, it appears likely that the lattice contribution will also depend strongly on rotation angles. Such a calculation of the lattice contribution is problematic, however, because one wants to consider the SOI-induced symmetry-breaking distortions away from a reference structure that is not itself an equilibrium structure in the absence of SOI. In principle it may be possible to compute these using an approach similar to that in Ref. 13. That is, one would compute the force-constant matrix and dynamical charges (in the absence of SOI) and the SOI-induced forces for a given configuration of octahedral rotations, and use these to predict the induced amplitudes of the infra-red-active phonon modes and the resulting lattice contribution to the polarization. We have not pursued such an approach here, as it would take us beyond the intended scope of the present work.

V. SUMMARY

We have used first-principles methods to compute the electronic and lattice contributions to the spin-orbit induced electric polarization in the cycloidal-spin compound TbMnO₃ with the spin spiral in the b - c and a - b planes. In the latter case we find that the electronic contribution is of the same order of magnitude as the lattice contribution, in strong contrast to previous studies of the b - c case.

We have studied the electronic contribution to the polarization in detail by considering a structural model based on rigid rotations of MnO₆ octahedra. We have shown that the electronic contribution to the polarization can change significantly with rotation angle even in the case of the b - c spiral, thus demonstrating that our previous neglect of this contribution was justified only because of an accidental property of the relaxed $Pbnm$ structure. We have introduced a phenomenological model that expands the electronic contribution to the polarization up to second order in the oxygen displacements from the Mn-Mn midbond positions, and have shown that it can explain the quite different behavior of the polarization in the b - c and a - b spiral cases.

Acknowledgments

This work was supported by NSF Grant DMR-0549198.

-
- * Electronic address: andreim@physics.rutgers.edu
- ¹ M. Fiebig, J. Phys. D: Appl. Phys. **38**, R123 (2005).
 - ² T. Kimura, Annu. Rev. Mater. Res. **37**, 387 (2007).
 - ³ D. I. Khomskii, J. Magn. Magn. Mater. **306**, 1 (2006).
 - ⁴ W. Eerenstein, N. D. Mathur, and J. F. Scott, Nature **442**, 759 (2006).
 - ⁵ S.-W. Cheong and M. Mostovoy, Nature Materials **6**, 13 (2007).
 - ⁶ Y. Tokura, J. Magn. Magn. Mater. **310**, 1145 (2007).
 - ⁷ B. Lorenz, Y.-Q. Wang, and C.-W. Chu, Phys. Rev. B **76**, 104405 (2007).
 - ⁸ S. Picozzi, K. Yamauchi, B. Sanyal, I. A. Sergienko, and E. Dagotto, Phys. Rev. Lett. **99**, 227201 (2007).
 - ⁹ C.-Y. Ren, Phys. Rev. B **79**, 125113 (2009).
 - ¹⁰ T. Kimura, T. Goto, H. Shintani, K. Ishizaka, T. Arima, and Y. Tokura, Nature **426**, 55 (2003).
 - ¹¹ T. Goto, T. Kimura, G. Lawes, A. P. Ramirez, and Y. Tokura, Phys. Rev. Lett. **92**, 257201 (2004).
 - ¹² H. J. Xiang, S.-H. Wei, M.-H. Whangbo, and J. L. F. Da Silva, Phys. Rev. Lett. **101**, 037209 (2008).
 - ¹³ A. Malashevich and D. Vanderbilt, Phys. Rev. Lett. **101**, 037210 (2008).
 - ¹⁴ A. Malashevich and D. Vanderbilt, Eur. Phys. J. B (2009), published online, DOI: 10.1140/epjb/e2009-00208-2.
 - ¹⁵ A “cycloid” is a special case of a “spiral” in which the magnetic moment is confined to a plane containing the wavevector.² All of the spiral configurations discussed in this manuscript are actually cycloidal.
 - ¹⁶ N. Aliouane, K. Schmalzl, D. Senff, A. Maljuk, K. Prokeš, M. Braden, and D. N. Argyriou, Phys. Rev. Lett. **102**, 207205 (2009).
 - ¹⁷ P. E. Blöchl, Phys. Rev. B **50**, 17953 (1994).
 - ¹⁸ G. Kresse and D. Joubert, Phys. Rev. B **59**, 1758 (1999).
 - ¹⁹ G. Kresse and J. Furthmüller, Comput. Mater. Sci. **6**, 15 (1996); Phys. Rev. B **54**, 11169 (1996).
 - ²⁰ S. L. Dudarev, G. A. Botton, S. Y. Savrasov, C. J. Humphreys, and A. P. Sutton, Phys. Rev. B **57**, 1505 (1998).
 - ²¹ R. D. King-Smith and D. Vanderbilt, Phys. Rev. B **47**, 1651 (1993).
 - ²² Y. Yamasaki, H. Sagayama, N. Abe, T. Arima, K. Sasaki, M. Matsuura, K. Hirota, D. Okuyama, Y. Noda, and Y. Tokura, Phys. Rev. Lett. **101**, 097204 (2008).
 - ²³ S. Baroni and P. Giannozzi, Rev. Mod. Phys. **73**, 515 (2001).
 - ²⁴ A. M. Glazer, Acta Crystallogr. Sect. B **B28**, 3384 (1972).
 - ²⁵ M. Cococcioni and S. de Gironcoli, Phys. Rev. B **71**, 035105 (2005).

²⁶ L. Hedin and S. Lundqvist, in *Solid State Physics*, edited by H. Ehrenreich, F. Seitz, and D. Turnbull (Academic, New York, 1969), vol. 23.

²⁷ A. Georges, G. Kotliar, W. Krauth, and M. J. Rozenberg, *Rev. Mod. Phys.* **68**, 13 (1996).